Synthesis and Doping of a Multifunctional Tetrathiafulvalene-Substituted Poly(isocyanide)

Elba Gomar-Nadal,[†] Laurent Mugica,[†] José Vidal-Gancedo,[†] Juan Casado,[‡] Juan T. López Navarrete,[‡] Jaume Veciana,[†] Concepció Rovira,[†] and David B. Amabilino*[,†]

Departament de Nanociència Molecular i Materials Orgànics, Institut de Ciència de Materials de Barcelona (ICMAB), Consejo Superior de Investigaciones Científicas (CSIC), Campus Universitari de Bellaterra, 08193 Cerdanyola del Vallès, Catalonia, Spain, and Department of Physical Chemistry, University of Málaga, Campus de Teatinos s/n, Málaga 29071, Spain

Received May 15, 2007; Revised Manuscript Received July 26, 2007

ABSTRACT: The poly(isocyanide) skeleton is shown to be a good support for assemblies of molecular units which permit p-type charge transport. A poly(isocyanide) containing tetrathiafulvalene (TTF) moieties in the side chains has been synthesized and characterized in its neutral state and has been oxidized to generate mixed valence states which display charge mobility in solution. UV−vis−NIR, EPR, and Raman spectroscopies were used to study the electronic properties of the polymer in its doped states, which were generated chemically with different oxidants. A broad charge-transfer band at 2100 nm characteristic of mixed valence agglomerations of neutral and cation radical TTFs was shown at lower doping levels, while evidence of aggregates between radical cation and the dicationic form of the heterocyclic system were seen at higher degrees of oxidation. The neutral macromolecule, the first mixed valence state, and the cation radical system can be reversibly interconverted by alternate oxidation with $Fe(ClO_4)_3$ and subsequent reduction with triethylamine, and therefore the material can be considered as a candidate for electrochromic switches. EPR measurements reveal magnetic interactions between cation radical TTF moieties as well as indication of charge delocalization over the macromolecule. Bearing in mind the steric impediment that the alkyl chains attached to the TTF unit provide, we conclude that the results suggest that the motion of the charges in the first mixed valence state is intramacromolecular: this hypothesis implies that there are interactions of the TTF residues in the side chains of the polymer which lead to a stack of the π-functional units, confirming the affirmation that this polymer skeleton is appropriate for appending electron-conducting stacks of π-functional units.

Introduction

Conducting "wires" with nanometer dimensions are potentially interesting materials as components in molecular electronic devices,[1] as witnessed by the spectacular achievements obtained in the field using carbon nanotubes.[2] There are at least three main ways for organic chemists to approach this type of functional material: (i) main-chain conducting polymers,[3] (ii) self-assembly of columns of π-functional components,[4] including DNA,[5] and (iii) side-chain functionalized polymers with π-functional monomers.[6] In all of these contexts, and especially in the latter two, the realization of conducting properties can only be obtained when the electroactive units are arranged in a precise spatial manner. Although the vast majority of conducting polymers present charge transport along their principal covalent skeleton, the use of a rigid neutral skeleton as a scaffold for side groups which upon doping present conductivity thanks to electron movement through noncovalent bonds is an interesting target, the one which is the objective of this work.

Examples of organic molecules with tendency to arrange themselves into stacks to maximize $\pi-\pi$ overlap are coronenes,[7] porphyrins,[8] phthalocyanines,[9] among others,[10] and electron conductivity has been described through these kind of $\pi-\pi$ stacks.[11] Tetrathiafulvalene (TTF) derivatives[12] also fall in this group of compounds, and a vast collection of crystals of conducting and superconducting charge-transfer salts and complexes exist.[13] The worth of the neutral donors in field effect transistors has also been demonstrated.[14] In addition, very recently the gel state has been used to organize the donors into conducting fibers.[15] Another way to organize these units is using a polymer skeleton as a scaffold, with stacks of the donor aligned roughly perpendicular to the main chain of the macromolecule. The poly(isocyanide)s[16] are attractive here because in some cases they present a rigid backbone that can be used to organize their side groups with a high degree of order[17] and the separation of these side groups (∼3.5 Å) is appropriate to have $\pi-\pi$ interactions between them[18] and thus provide a path for electron transport when charge is generated in the stack (Figure 1). The regular 4_1 helix is not necessarily the energy minimum, and several conformations are possible in the polymer backbone[19] with other types of helix possible,[20] which might lead to irregular structures and result in charge localization. We will show here that this possible drawback does not impede interesting properties being observed in the polymers.

The preparation of TTF-containing side-chain poly(isocyanide)s appealed to us, because mixed valence stacks of these units can give rise to conductivity in crystals. A number of polymers have been prepared which contain the TTF unit either in the main chain[21] or the side chain.[22] Most of the former TTF-based polymers have been poorly characterized on account of their low solubilities. On the other hand, the second kind of polymers present flexible spacers to attach the TTF units to the polymer skeleton giving rise to a lot of possible conformations that make difficult their controlled organization, leading to

* Corresponding author. Tel.: 34935801853. Fax: 34935805729. E-mail: amabilino@icmab.es.
[†] Institut de Ciència de Materials de Barcelona (ICMAB).
[‡] University of Málaga.

10.1021/ma0710986 CCC: $37.00
Published on Web 09/25/2007

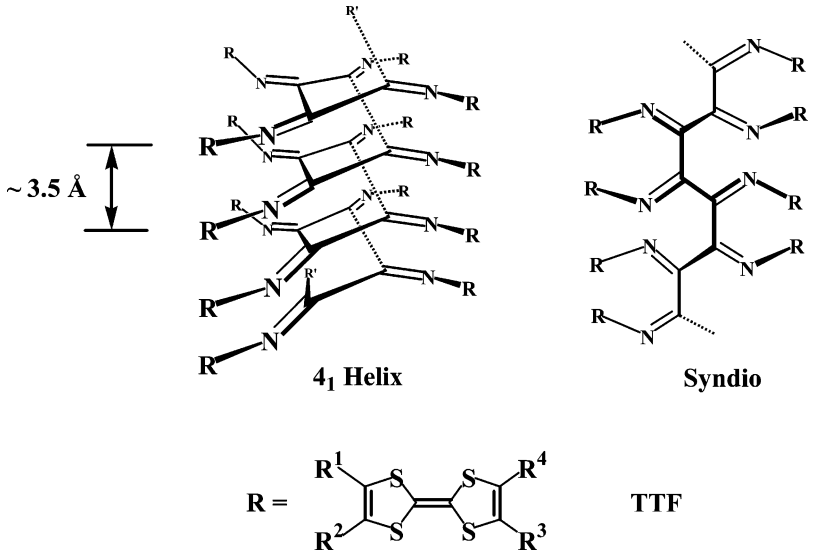

Figure 1. Cartoon representation of the 4_1 helix structure that would favor $\pi-\pi$ stacking of TTF units in the side chains of the polymer and the syndio conformation of the same poly(isocyanide).

Scheme 1[a]

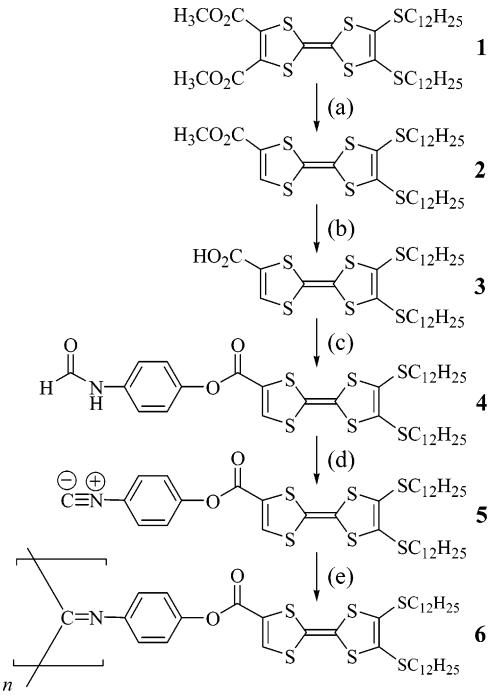

[a] Conditions: (a) LiBr, HMPA, 80 °C, 75%; (b) $LiOH\cdot H_2O$, H_2O, THF, 99%; (c) *N*-4-hydroxy-phenyl-formamide, DCC, DMAP, CH_2Cl_2, 70%; (d) $ClCO_2CCl_3$, NEt_3, CH_2Cl_2, 75%; (e) catalyst (see Table 1), CH_2Cl_2, 65−85%.

localized dimers rather than continuous stacks. This last problem would be overcome if the poly(isocyanide)'s skeleton adopted a rigid secondary structure and the presence of long alkyl chains would have a triple function: (i) increase the solubility of the polymer, (ii) act as an insulating mantle around the macromolecule as in electrical cables, and (iii) act as a "fastener" for the TTF moieties because of van der Waals interactions between them.[23]

This article describes the synthesis, characterization, and detailed doping study of a novel poly(isocyanide) bearing TTF derivatives in its side chains (Scheme 1) that reveals the existence of charge delocalization between TTF units in the macromolecule. Recently, we demonstrated that a related optically active TTF-based polymer can act as multistate chiroptical redox switch,[24] and the polymer also displays electrochromic behavior with multiple states. In addition we show atomic force microscope studies of the new polymer, which provides important information regarding the consequences of monomer design for the preparation of materials of this type.

Experimental Section

Materials and Methods. *N*-(4-Hydroxy-phenyl-formamide[25] and 2,3-bis(dodecylthio)-6,7-bis(methoxycarbonyl)tetrathiafulvalene[26] (**1**, Scheme 1) were synthesized using procedures reported in the literature. All other chemicals were commercially available and were used as obtained. Tetrahydrofuran (THF) was distilled over sodium/benzophenone and CH_2Cl_2 over P_2O_5. Thin-layer chromatography (TLC) was performed on aluminum plates coated with Merck silica gel 60 F254. Developed plates were air-dried and scrutinized under a UV lamp. Silica gel 60 (35−70 mesh, SDS) was used for column chromatography. Melting points were determined using a Melting Point SMP10, BIBBY Stuart Scientific instrument and are uncorrected. Laser desorption/ionization time-of-flight mass spectra (LDI-TOF-MS) were obtained using a Kratos Kompact Maldi 2 K-probe (Kratos Analytical) or a Voyager-DE RP (PerSeptive Biosystems) operating with pulsed extraction of the ions in positive and linear high-power mode. The samples were deposited directly onto a nonpolished stainless steel sample plate from CH_2Cl_2 solution. Infrared spectra were recorded on a Perkin-Elmer FT-IR Spectrum One spectrometer. ^1H and ^{13}C NMR spectra were obtained using a Bruker Avance 250 spectrometer with deuterated solvent as lock and tetramethylsilane as internal reference. UV−vis spectra were recorded using a Varian Cary 05E spectrophotometer.

Cyclic voltammograms were recorded with the conventional three-electrode configuration in CH_2Cl_2 containing 0.1 M $[NBu_4][PF_6]$, as a supporting electrolyte, with Pt electrodes and a Ag/AgCl electrode as a reference one. Gel permeation chromatography (GPC) was performed using a Shimadzu SCL-10A chromatograph equipped with two Supelco Progel TSK columns (G3000-HXL and G4000-HXL, 7.8 mm i.d. × 30 cm), in series and protected by a Supelco Progel TSK guard column (HXL-H). THF solutions of the polymer (50 μL, 1 mg/l) were introduced, the THF eluent was pumped at 1 $mL\cdot min^{-1}$ with a Shimazu LC10AT pump and registered using a Shimazu SPD-M10AVP detector. The molecular masses were determined against polystyrene standards.

Electron paramagnetic resonance (EPR) spectra were obtained on a Bruker ESP-300E spectrometer operating at X-band (9.3 GHz), equipped with a rectangular cavity, T 102. The signal-to-noise ratio was increased by accumulation of scans using the F/F lock

accessory, Bruker ER 033M, and an NMR gauss meter, Bruker ER 0035M, to guarantee a high-field reproducibility. Precautions to avoid undesirable spectral line broadening such as that arising from microwave power saturation and magnetic field overmodulation were taken.

Atomic force microscopy (AFM) experiments were performed using a PicoSPM from Molecular Imaging. Solutions of polymer in CH_2Cl_2 or $CHCl_3$ were drop-cast onto freshly cleaved highly oriented pyrolytic graphite (HOPG, quality ZYB from GE Advanced Ceramics). All images were taken in acoustic mode in air at room temperature. Commercial acoustic mode tips (FM from Nanosensors) were used with a typical force constant of 1.2−5.5 $N \cdot m^{-1}$ and resonance frequency of around 60−100 kHz.

FT-Raman spectra were measured by use of the FT-Raman accessory kit (FRA/106-S) of a Bruker Equinox 55 FT-IR interferometer. A continuous wave Nd:YAG laser working at 1064 nm was employed for Raman excitation. A total of 3000 scans were averaged in each spectrum obtained with laser power lower than 15 mW.

2,3-Bis(dodecylthio)-6-(methoxycarbonyl)tetrathiafulvalene (2). A solution of 2,3-bis(dodecylthio)-6,7-bis(methoxycarbonyl)tetrathiafulvalene[26] (**1**, 723 mg, 1.016 mmol) and LiBr (975 mg, 11.226 mmol) in hexamethyl phosphoramide (HMPA) (10 mL) with a drop of H_2O was heated to 80 °C, causing evolution of gas (CH_3Br). When no more gas evolved, the mixture was cooled to room temperature, H_2O (10 mL) was added, and the resulting solution was cooled to −5 °C. The orange solid that separated was filtered and washed with water, dissolved in CH_2Cl_2, and the solution was subsequently dried over $MgSO_4$, treated with active charcoal, and evaporated to dryness, leaving an orange solid that was crystallized from a mixture of CH_2Cl_2/MeOH (538 mg, 80%) and characterized as **2**. LDI-TOF-MS *m*/*z* (%): 662.4 (M^+, 100); calcd for $C_{32}H_{54}O_2S_6$ 662.4. Mp 55−58. FT-IR (cm^{-1}, KBr): 3098 (w), 2956 (m), 2919 (s), 2848 (s), 1726 (m, C═O), 1711 (m, C═O), 1568 (w), 1537 (w), 1466 (m), 1435 (w), 1384 (w), 1256 (s, C−O), 1200 (w), 1053 (w), 943 (w), 892 (w), 833 (w), 804 (w), 764 (w), 728 (w), 662 (w). ^{1}H NMR (250 MHz, $CDCl_3$): 7.38 (s, 1H, C═C*H*), 3.84 (s, 3H, $-CO_2CH_3$), 2.84 (t, J = 7.3 Hz, 2H, $-SCH_2(CH_2)_{10}$), 2.83 (t, J = 7.3 Hz, 2H, $-SCH_2(CH_2)_{10}$), 1.65 (c, J = 7.5 Hz, 4H, $-SCH_2CH_2$), 1.5−1.2 (m, 36H, $-S(CH_2)_2(CH_2)_9$), 0.91 (t, J = 6.5 Hz, 6H, $-CH_2CH_3$) ppm. ^{13}C NMR (62.8 MHz, $CDCl_3$): 159.8 ($-CO_2CH_3$), 133.0 ($-CCO_2CH_3$), 128.4 and 128.2 ($-CSCH_2$), 127.5 (−CH), 111.8 and 110.1 (central C═C), 52.7 ($-CO_2CH_3$), 36.4, 32.0, 29.8, 29.8, 29.7, 29. 7, 29.6, 29.5, 29.3, 29.1 and 28.5 ($-S(CH_2)_{10}$), 22.7 ($-CH_2CH_3$), and 14.1 ($-CH_2CH_3$) ppm.

2,3-Bis(dodecylthio)-6-(carboxy)tetrathiafulvalene (3). $LiOH \cdot H_2O$ (153 mg, 3.646 mmol) in 5 mL of H_2O was added dropwise to a stirred solution of bis(dodedecylthio)-6-(methoxycarbonyl)-tetrathiafulvalene (**2**, 180 mg, 0.271 mmol) in THF (20 mL). After stirring for 12 h, the mixture was diluted with ether (25 mL) and hydrochloric acid (0.5 M, 10 mL) was added. The dark organic phase was dried ($MgSO_4$), and the resulting purple solid (174 mg, 99%) was characterized as **3**. Calcd for $C_{31}H_{52}O_2S_6$; C 57.36, H 8.07, S 29.64; exptl. C 57.09, H 8.44, S 29.94. LDI-TOF-MS *m*/*z* (%): 648.3 ($[M]^+$ 60) and 604.3 ($[M-CO_2H]^+$, 100); calcd 648.2. Mp 96−97. FT-IR (cm^{-1}, KBr): 3700−3200 (w, br, OH), 2955 (m), 2920 (s), 2850 (m), 1668 (m, C═O), 1562 (w), 1531 (w), 1467 (w), 1422 (w), 1297 (w), 1201 (w), 1045 (w), 888 (w), 848 (w), 819 (w), 773 (w), 727 (w), 673 (w), 501 (w). ^{1}H NMR (ppm, 250 MHz, $CDCl_3$): 7.51 (s, 1H, $-CO_2H$), 7.01 (s, 1H, C═C*H*), 2.84 (t, br, 4H, $-SCH_2$), 1.65 (c, J = 6.7 Hz, 4H, $-SCH_2CH_2$), 1.50−1.20 (m, 36H, $-S(CH_2)_2(CH_2)_9$), 0.91 (t, J = 6.5 Hz, 6H, $-CH_3$) ppm.

(Formylamino)phenyl (2,3-Bis(dodecylthio)-6-(carboxy)tetrathiafulvalene (4). A solution of 2,3-bis(dodecylthio)-6-(carboxy)-tetrathiafulvalene (**3**, 200 mg, 0.31 mmol), *N*-(4-hydroxy-phenyl-formamide[25] (59 mg, 0.43 mmol), 1,3-dicyclohexylcarboiimide (DCC, 102 mg, 0.49 mmol), and a few small crystals of 4-dimethylaminopyridine (DMAP) in CH_2Cl_2 (6 mL) was stirred overnight under a $CaCl_2$ guard tube. The originally red solution changed to orange with a white precipitate in suspension that was separated by filtration and washed with CH_2Cl_2. The filtrate was extracted with NaOH (2%, 2 × 50 mL) and H_2O (2 × 50 mL). The resulting organic phase was dried over $Na_2(SO_4)$, filtered, and evaporated to dryness, leaving an orange solid (297 mg) which was purified by flash column chromatography (silica gel, CH_2Cl_2/EtOAc 19:1) obtaining 162 mg (70%) of an orange solid characterized as **4**. Elemental Anal. Calcd for $C_{38}H_{57}NO_3S_6$: C 59.41, H 7.48, N 1.82, S 25.04. Exptl.: C 58.94, H 7.56, N 1.76, S 25.07. LDI-TOF-MS *m*/*z* (%): 767.3 (M^+, 100); calcd 767.2. Mp 96−97. FT-IR (cm^{-1}, KBr): 3346 (m, NH), 2919 (s), 2848 (m), 1743 (s, C═O), 1664 (s, C═O), 1567 (w), 1526 (m), 1464 (m), 1407 (w), 1232 (s), 1194 (w), 1151 (w), 849 (w), 718 (w). ^{1}H NMR (250 MHz, $CDCl_3$): 8.64 (d, J = 11.2 Hz, 0.5H, $-CHO$ trans with respect to $-NH-$), 8.34 (d, J = 1.7 Hz, 0.5H, C*H*O cis with respect to $-NH-$), 8.12 (d, J = 11.2 Hz, 0.5H, $-NH-$ trans with respect to $-CHO$), 7.40−7.60 (m, 3.5H, $-NH-$ cis with respect to $-CHO$, $-H_{ortho}$ to −NHCHO and C═C*H*), 7.06−7.17 (m, 2H, $-H_{ortho}$ to −OR), 2.82 (t, J = 7.3 Hz, 4H, $-SCH_2$), 1.63 (c, J = 7.2 Hz, 4H, $-SCH_2CH_2$), 1.50−1.10 (m, 36H, $-S(CH_2)_2(CH_2)_9$), 0.88 (t, J = 6.5 Hz, $-CH_3$) ppm. ^{13}C NMR (62.8 MHz, $CDCl_3$): 162.4 ($-CO_2R-$), 158.9 and 157.8 (cis and trans −NH*C*HO), 147.5, 146.7, 135.0, 134.8, 134.5, 134.3, 128.5, 127.5, 127.4, 127.3, 122.7, 121.9, 121.0, 120.0, 111.3, 111.1, 111.0 and 110.8 (*C*═*C*), 36.4, 31.9, 29.8, 29.8, 29.7, 29.7, 29.6, 29.5, 29.5, 29.1 and 28.5 ($-S(CH_2)_{10}$), 22.7 ($-CH_2CH_3$), 14.1 ($-CH_3$) ppm.

Benzene (2,3-Bis(dodecylthio)-6-(carboxy)tetrathiafulvalene)-4′-isocyanide (5). A solution of diphosgene (14 μL, 0.116 mmol) in CH_2Cl_2 (1 mL) was added dropwise to a solution of (formylamino)phenyl (2,3-bis(dodecylthio)-6-(carboxy)tetrathiafulvalene (**4**, 80 mg, 0.104 mmol) and NEt_3 (40 μL, 287 mmol) in CH_2Cl_2 (4 mL) at −5 °C. An immediate change in color from orange to red was observed. After stirring for 1 h, the mixture was diluted with CH_2Cl_2 (20 mL) and $NaHCO_3$ (aq, 10%, 10 mL) was added. The organic phase was extracted with $NaHCO_3$ (aq, 10%, 10 mL, 2 × 20 mL) and H_2O (2 × 20 mL), dried with $Na_2(SO_4)$, filtered, and evaporated to dryness, leaving a red solid (89 mg) which was purified by flash column chromatography (silica gel, CH_2Cl_2) obtaining 56 mg (75%) of a red solid characterized as **5**. LDI-TOF-MS *m*/*z* (%): 750.9 ($[M]^+$, 60); calcd for $C_{31}H_{52}O_2S_6$ 750.2 $g \cdot mol^{-1}$. FT-IR (cm^{-1}, KBr): 2918 (s), 2849 (m), 2121 (m, C≡N), 1703 (s, C═O), 1561 (w), 1528 (w), 1496 (m), 1469 (w), 1300 (w), 1270 (m), 1201 (w), 1220 (w), 1100 (m), 840 (w), 819 (w), 718 (m), 520 (w). ^{1}H NMR (250 MHz, $CDCl_3$): 7.60 (s, 1H, C═C*H*), 7.43 (m, 2H, H_{ortho} with respect to −OR), 7.21 (m, 2H, H_{ortho} with respect to −NC), 2.82 (t, J = 7.2 Hz, 4H, $-SCH_2$), 1.63 (c, J = 7.2 Hz, 4H, $-SCH_2CH_2$), 1.50−1.10 (m, 36H, $-S(CH_2)_2(CH_2)_9$), 0.88 (t, J = 6.5 Hz, $-CH_3$) ppm. ^{13}C NMR (62.8 MHz, $CDCl_3$): 165.2 ($-CO_2R$), 156.9 ($-CN$), 150.4, 135.1, 128.5, 127.8, 127.5, 127.0, 124.5, 122.6 and 111.7 (*C*═*C*), 36.4, 31.9, 29.8, 29.7, 29.5, 29.4, 29.1 and 28.5 ($-S(CH_2)_{10}$), 22.7 ($-CH_2CH_3$), 14.1 ($-CH_3$) ppm.

Poly{Benzene (2,3-Bis(dodecylthio)-6-(carboxy)tetrathiafulvalene)-4′-isocyanide} (6). A catalyst (see Table 1) solution (0.04 mol/L) in MeOH was added to a solution of the monomer **5** (25 mg/mL) in CH_2Cl_2 such that the ratio mol catalyst/mol monomer was 1:100. The mixture was stirred for 20 h and was poured into MeOH. The precipitate was collected by filtration and washed with MeOH to give polymer **6** as an orange solid (65−85%, see Table 1). FT-IR (cm^{-1}, KBr): 2953 (m), 2922 (s), 2851 (s), 1720 (m, C═O), 1642 (w, >C═NR), 1562 (m), 1493 (m), 1562 (m), 1532

Table 1. Yields and Molecular Weight Distributions of Polymer 6 Prepared Using Different Ni(II) Salts as Catalysts

catalyst	yield (%)	$\bar{M}_n$ (kDa)	$\bar{M}_w$ (kDa)	$\bar{M}_z$ (kDa)	Q^a
$NiCl_2 \cdot (H_2O)_6$	85	27.3	65.0	148.6	2.4
$Ni(ClO_4)_2 \cdot (H_2O)_6$	65	34.7	74.9	153.6	2.2
$Ni(Acac)_2$	85	26.2	127.5	372.8	3.5
$Ni(Py)_4Cl_2$	70	33.8	94.1	238.5	2.8

[a] Polydispersity. Acac = acetylacetonate, and Py = pyridine.

(w), 1493 (m), 1465 (m), 1415 (w), 1376 (w), 1267 (s), 1229 (s), 1184 (s), 1098 (w), 1013 (m), 882 (m), 850 (w), 833 (w), 772 (w), 719 (w) 525 (w). ^{1}H NMR (250 MHz, $CDCl_3$): 7.60−5.00 (br, 5H, C═C*H* and −H_{arom}), 2.86 (br, 4H, −SCH_2), 1.66 (br, 4H, −S$CH_2C H_2$), 1.50−1.10 (br, 36H, −S$(CH_2)_2(CH_2)_9$), 0.88 (br, 6H, −CH_3) ppm. ^{13}C NMR (62.8 MHz, $CDCl_3$): 160−165 (br, −CO_2R i, >*C*═NR), 158−155, 150−145, 138−132, 129−127, 124−117 and 113−108 (br, *C*═*C*), 36.4−36.6, 32.0, 30.0−29.50 and 28.9−28.5 (−S$(CH_2)_{10}$), 22.8 (−CH_2CH_3), 14.2 (−CH_3) ppm.

Doping of Poly(isocyanide) 6. The oxidation of the polymer was followed recording UV−vis−NIR and EPR spectra of fractions with different doping degree. These fractions were prepared by adding oxidant solution (10^{-3} to 10^{-2} M) to a solution of the poly(isocyanide) **6** (0.5 mL, 1.5×10^{-3} M) placed in a 5 mL volumetric flask that is filled up to the calibration mark with the solvent after the addition. This procedure results in a new solution with an appropriate concentration (10^{-4} M) to use cells of 1 cm optical path. The solvent used for the oxidation with $Fe(ClO_4)_3$ was CH_2Cl_2/CH_3CN 7:3 and that for Br_2 and I_2 was CH_2Cl_2. The UV−vis−NIR baseline was recorded using the solvent. The absorbance of $Fe(ClO_4)_3$ (357 nm) is negligible in the working range of concentration used and important up to a certain point for Br_2 (444 nm, see text) and I_2 (490 nm).

Results and Discussion

Synthesis and Characterization of the Polymer. The synthetic route used for the preparation of poly(isocyanide) **6** is depicted in Scheme 1. Treatment of 2,3-bis(dodecylthio)-6,7-bis(methoxycarbonyl)tetrathiafulvalene (**1**)[26] with LiBr and HMPA at 80 °C gave the monodecarboxymethylated product **2**. Basic hydrolysis of **2** led to the acid **3**, which was coupled with *N*-4-hydroxy-phenyl-formamide[25] using DCC in the presence of DMAP at afford formamide **4**. Dehydration of **4** with diphosgene gave isocyanide **5**. The conversion of the formamide to the isocyanide was evidenced by symmetrization in the NMR spectra[27] as well as by the characteristic IR band (at 2121 cm^{-1}) arising from the isocyanide moiety.

The poly(isocyanide) **6** was prepared (Scheme 1) in CH_2Cl_2, using different Ni(II) salts as catalysts (see Table 1), at a concentration of isocyanide monomer of approximately 150 mM. Air was allowed to be present during the reaction, as it has been shown to be involved during the catalysis in polymerizations of this type.[28] The polymerizations proceed in good yields in all cases tried, ranging from 65% for perchlorate up to 85% for chloride and acetylacetonate salts (Table 1). Gel permeation chromatography gave polydispersity values between 2.4 and 3.5, higher than for other aromatic poly(isocyanide)s generated using Ni(II) salts but with molecular weights of similar order. The reason for these characteristics with this monomer system is not clear at present, although the size of the monomer may be an influence (the molecular mass is approximately 750 Da).

Differential scanning calorimetry (DSC) and thermogravimetric analysis (TGA) of the solid amorphous polymer **6** showed no significant phase transitions in the range of 40−200 °C, but all samples decomposed (weight loss from sample witnesses by TGA) above approximately 230 °C in air. The polymer is very soluble in organic solvents such as toluene, CH_2Cl_2, $CHCl_3$, and THF, whereas it shows low solubility in hexane, CH_3CN, and short-chain alcohols, and remains insoluble in water.

The spectroscopic characteristics of the polymers prepared using different catalysts were essentially identical. The IR spectra gave a broad band from the imine groups attached to the polymer backbone at approximately 1639 cm^{-1} and no signal corresponding to the isocyanide moiety. The ^{1}H NMR spectra contained extremely broad resonances in the aromatic region from approximately 8.0 to 5.5 ppm corresponding to the phenyl moiety and the −CH part of the TTF unit. The high-field position of the resonances arising from the aromatic groups, seen before in this type of polymer,[29] is indicative of the proximity of the aromatic groups. The hydrogen atoms close to the polymer backbone present broad peaks, whereas those from the atoms in the aliphatic solubilizing groups of the macromolecule are more well-resolved, reflecting the higher mobility of the atoms at the end of the side chain. The ^{13}C NMR spectra reveal similar characteristics to the ^{1}H NMR spectra with broad resonances arising from carbon atoms close to the polymer skeleton. In particular, the resonance arising from the carbon atoms in the skeleton itself is extremely broad (see the Supporting Information), indicating the sterically hindered nature of the polymer core.

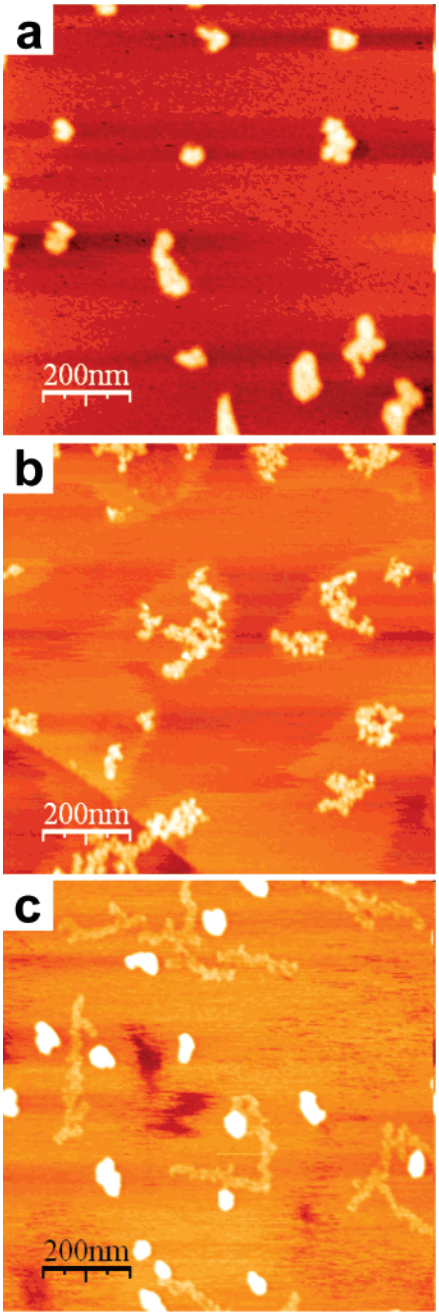

Figure 2. AFM images of polymer **6** obtained by drop-casting of a solution (10^{-6} to 10^{-7}) M in CH_2Cl_2 or $CHCl_3$ on graphite: (a) compact islands, (b) islands with substructure and, (c) mixture of islands and worms.

Table 2. Redox Potentials of Polymer 6 and Precursor 4 and Comparison of the Number of Oxidant Equivalents Needed to Have the Same Degree of Oxidation with $Fe(ClO_4)_3$, Br_2, and I_2

				UV−vis band evolution (no. of oxidant equiv/1 TTF equiv)			
	potentials (V)[a]			2100 nm		∼770 nm	∼620 nm
compd	$E_{1/2}(0/\cdot+)$	$E_{1/2}(\cdot+/2+)$	oxidant	max[b]	dis.[b]	max[b]	max[b]
4	0.64	1.07	$Fe(ClO_4)_3$			∼1.0	∼2.0
			Br_2			∼6.7	>60
6	0.64	1.02	$Fe(ClO_4)_3$	∼0.5	∼1.0	∼1.0	∼2.3
			Br_2	∼0.5	∼4.0	∼6.7	>60
			I_2	∼24	>60	>60	>60

[a] Versus Ag/AgCl recorded with $[NBu_4][PF_6]$ in CH_2Cl_2. [b] max = maximum of absorption of this band, and dis. = disappearance.

The shape characteristics of the neutral macromolecule were studied by AFM on a graphite substrate from dilute solutions in CH_2Cl_2 and $CHCl_3$, using the acoustic mode to image. (Contact mode could not be used to image the macromolecules because the polymer−surface interaction is so low that the microscope tip wipes the sample away.) At high concentrations (10^{-5} M, not shown) a monolayer of polymer was observed, with no well-defined morphology. Upon dilution (10^{-6} to 10^{-7} M), three different kinds of image were recorded: (i) compact islands (Figure 2a), (ii) islands with substructure (Figure 2b), and (iii) a mixture of islands and worms (Figure 2c). The last class of image was seen much less frequently than the other two types. Further dilution (10^{-7} to 10^{-8} M) did not result in any change in the main features. The measured height of the islands was 4−6 nm, and that of the worms was 0.8−1.3 nm. The former range of height is consistent with the theoretical width of the polymer with alkyl chains extending from the backbone (6 nm for the totally extended model depicted in Figure 1). On the basis of the molecular weight calculated by GPC (see Table 1), the polymer length should be between 14 and 30 nm,[30] so the wormlike figures are clearly aggregates of macromolecules, and no isolated polymer molecules were observed. Experiments performed using hexane, toluene, or mixtures of CH_2Cl_2 with CH_3CN or MeOH as a solvent gave images composed for polymer aggregates of larger dimensions.

The results obtained for this polymer contrast markedly with the general impression obtained from AFM measurements of amino acid derived poly(isocyanide)s[31] which are considered to be shape persistent.[32] The amino acids permit hydrogen bonds between the monomer units in the backbone, which ensure a very high molecular weight in the polymer as well as that the rigid conformation leads to a rod that is not easily bent: fiberlike single molecules with large shape persistence have been observed by AFM. Also shorter hydrophilic poly(isocyanide)s have been observed in an extended conformation using the same technique.[33] On the other hand, it is known that stiff conjugated polymers with chemical defects can collapse into more compact cylindrical topographies.[34] From the AFM images obtained here, its seems that the backbone of the polymer **6** is either not as rigid as other macromolecules of this family, as has been suggested on other occasions for aliphatic poly(isocyanide)s in a different context,[35] or that the backbone of the polymer contains many defects. In this sense, it is worth pointing out that adjacent imine units can adopt the same or different conformations,[29,33] leading to isotactic, syndiotactic, or even atactic chains, and defects of this type could well lead to a folding up of the polymer segments (islands in Figure 2) or even to produce a nonhelical polymer (worms in Figure 2c). Indeed, the broadness of the imine carbon atom resonance in the ^{13}C NMR spectra may point to a nonisotactic situation, although again it should be stressed that the AFM images are a reflection of aggregates of molecules rather than isolated macromolecules.

Doping of the TTF-Containing Poly(isocyanide). The appearance of metallic conductivity in cation radical salts of TTF derivatives requires structurally regular intrastack mixed valence (MV) states, whereas an integer valence generally results in insulating materials.[36] In the case of polymer **6**, the main requisite is to have an adequate packing arrangement of the TTF groups in the polymer allowing mixed valence interactions after its doping and hence intrastack conduction. In this regard, cyclic voltamperommetry and UV−vis−NIR and EPR spectroscopies provide very useful information to analyze the formation of MV and univalent (UV) species with pillars of TTF units.

The electrochemical properties of polymer **6** were studied with CV. Two sequential and quasi-reversible waves at 0.64 and 1.02 V (vs Ag/AgCl recorded in $[NBu_4][PF_6]$ in CH_2Cl_2) characteristic of the presence of TTF groups in the side chains of the polymer are observed (that can be ascribed to the oxidation of the moiety to the corresponding cation radical and dication species, respectively). The oxidation potentials observed for the precursor **4**[37] under the same experimental conditions are very similar (Table 2), but its CV presents narrower redox waves due to its easier diffusion and unique chemical nature (the polymer contains a variety of TTF environments because of their different positions in the chains).

Polymer **6** has three extreme univalent states (like the monomer) and additionally two very broad mixed valence states (Figure 3). In the first univalent state all the TTF units are neutral (UVS1), the second has all TTF units as cation radicals (UVS2), and the most oxidized state has dications (UVS3). The mixed valence states are a mixture of neutral TTF and cation radical (MVS1) or cation radical and dication TTFs (MVS2). Note that no additional redox waves between the cation radical and dication TTF species are observed in the CVs, unlike those described for poly(thiophene)s with TTF units in the side chains—and attributed to the formation of MV dimers of neutral and cation radical TTFs ($TTF^0-TTF^{\bullet+}$).[38] Therefore, isolated dimers of mixed valence character are not present to any significant degree in the poly(isocyanide).

Polymer **6** was conveniently doped chemically using different oxidizing agents (Table 3), and evidence of the stoichiometry of the reactions was obtained by performing UV−vis absorption and EPR spectra. The best oxidizing agents found were, from most to least efficient, $Fe(ClO_4)_3$, bromine, and iodine. All resulted in the formation of the TTF cation radical, but the dication was only efficiently formed with the iron salt. Indeed, $Fe(ClO_4)_3$ allows a complete and practically quantitative oxidation of poly(isocyanide) **6** from the neutral to the fully dicationic state. The evolution of UV−vis−NIR absorption bands of polymer **6** (Figure 4) upon reaction with this salt show that the oxidation is accompanied by a very pronounced change in color

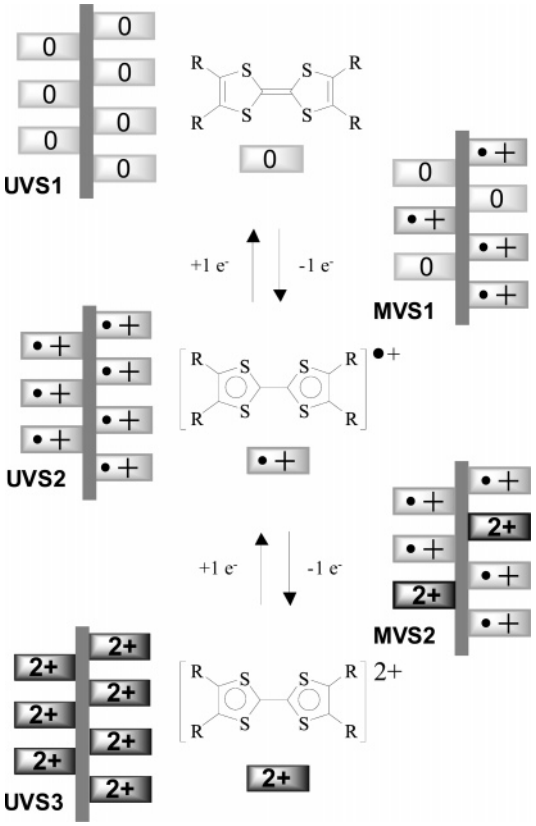

Figure 3. Cartoon representation of the redox states of polymer **6** with TTF units in the side chains that can be interconverted through redox reactions: univalent states with all neutral (UVS1), all cation radical (UVS2), or all dication (UVS3) TTF units, and the intermediate mixed valence states (MVS1 and MVS2).

Table 3. Oxidants' Activity toward Polymer 6

oxidant	solvent	effective
$Ag(NO_3)$	CH_2Cl_2/CH_3CN	no
$Ag(OCOCF_3)$	CH_2Cl_2/CH_3CN	no
TCNQ[a]	CH_2Cl_2	no
$Fe(ClO_4)_3$	CH_2Cl_2/CH_3CN	yes
Br_2	CH_2Cl_2	yes
I_2	CH_2Cl_2	yes

[a] TCNQ: tetracyano-*p*-quinodimethane.

of the solution that goes from the orange of the neutral state (UVS1) via green for the cation radical (UVS2), to the fully oxidized dicationic blue form (UVS3). Silver(I) salts—$Ag(NO_3)$ and $Ag(OOCCF_3)$—and tetracyano-*p*-quinodimethane (TCNQ) were not able to oxidize the polymer, probably because their oxidation potentials are similar or lower to the polymer ones under the conditions assayed.[39]

The neutral polymer (UVS1) has a weak and poorly defined absorption band at 450 nm (Figure 4a). The progressive addition of $Fe(ClO_4)_3$ leads to the formation of new bands at 2100, 930, 770, and 410 nm (Figure 4) characteristic of MVS1. The band at 2100 nm—which corresponds to charge transfer in mixed valence TTF stacks containing neutral and cation radical species—can be viewed as an anticipation of the optical conduction band observed in the reflectance spectrum of metallic TTF cation radical salts,[40] and it has also been seen in poly(thiophene)s that contain TTF derivatives in the side chains at slightly shorter wavelengths (1800 nm)[38] as well as other TTF-based polymers.[21] This band (which was not observed when the precursor **4** was oxidized under the same conditions) has a maximum absorption after addition of 0.5 equiv[41] of oxidant—the point at which there is an equal proportion of neutral and

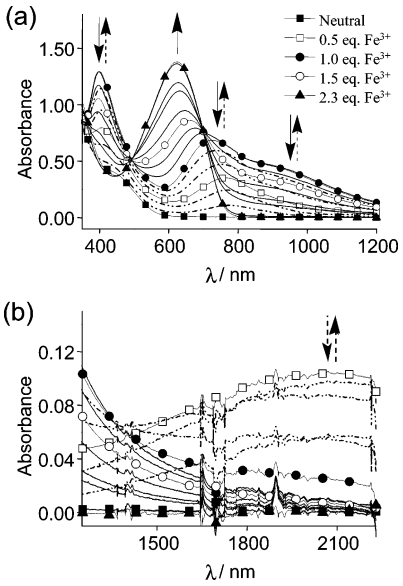

Figure 4. UV−vis−NIR absorption spectra that show the evolution of the oxidation of polymer **6** in CH_2Cl_2/CH_3CN 7:3 adding stoichiometric amounts of $Fe(ClO_4)_3$: (a) from 350 to 1200 nm and (b) from 1200 to 2230 nm. Arrows and spectra depicted with dashed lines represent the evolution of the bands between 0 and 1 equiv of oxidant and the solid ones between 1 and ~2 equiv.

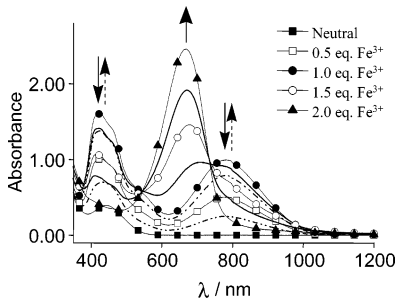

Figure 5. UV−vis−NIR absorption spectra that show the evolution of the oxidation of **4** in CH_2Cl_2/CH_3CN 7:3 adding $Fe(ClO_4)_3$. Arrows and spectra depicted with dashed lines represent the evolution of the bands between 0 and 1 equiv of oxidant and the solid ones between 1 and 2 equiv. No absorption bands are observed above 1200 nm in the near-IR.

cation radical TTFs—and disappears completely after the addition of ~1 equiv of $Fe(ClO_4)_3$—when all the TTFs are in their cation radical form (UVS2 in Figure 3). The absorption bands at 410, 770, and 930 nm have a maximum intensity at this stoichiometry and progressively decrease in intensity upon further addition of oxidant—while another band at 620 nm, characteristic of the dication TTF, appears—until their disappearance when slightly more than 2 equiv of the iron salt are added. These bands are characteristic of the TTF cation radical and its congregated forms. The assignment of each of these bands to single cation radical TTF or a group of them is not trivial.[42,43] When the absorption spectra of the oxidation process of the TTF **4** with that of the polymer one are compared, the bands at 930 nm (not seen for the precursor **4**, Figure 5) can be attributed to the formation of cation radical TTF stacks. The assignation of this band is clearer when considering the evolution of its absorption with respect to the band at 770 nm (characteristic of single cation radical TTF)[42] versus the number of equivalents of oxidant added (Figure 6). The absorption of this band does not increase at the same rate as that of the band at 770 nm, although its maximum absorption is at around 1 equiv of oxidant, which indicates that it is due to the absorption of other species such as stacks of cation radicals.[43] This hypothesis

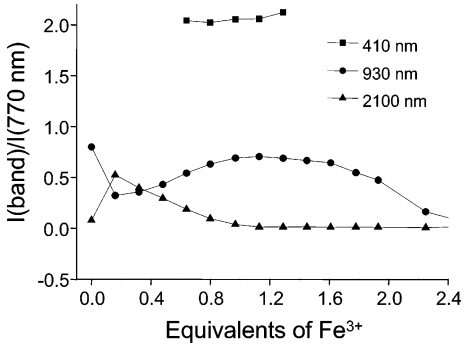

Figure 6. Plot of the normalized intensity with respect to the band at 770 nm for the bands at 410, 930, and 2100 nm vs the no. of equiv of Fe^{3+}.

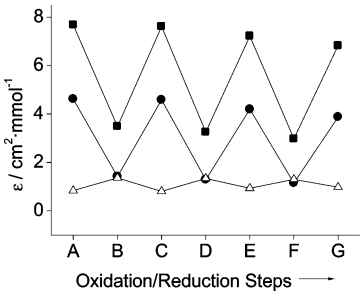

Figure 7. Alternating oxidations and reductions carried out for polymer **6** in CH_2Cl_2/CH_3CN using $Fe(ClO_4)_3$ as an oxidant and NEt_3 as a reducing agent. Absorption coefficient (ϵ) changes associated with the bands at 720 (■), 930 (●), and 2100 nm (△) after adding 1 equiv of $Fe(ClO_4)_3$ (step A) to a solution of neutral polymer and continuing with the alternative addition of proportions of 1.6 mol of NEt_3 (steps B, D, F) and 0.5 equiv of $Fe(ClO_4)_3$ (steps C, E, G) to the resulting solution.

is also supported by the EPR studies (vide infra). The observation of a band characteristic of cation radical stacks is another proof that the TTF units in the side chains of the polymer are interacting closely.

A priori, the formation of MV and cation radical stacks could arise from intra- or intermacromolecular interactions. However, the strong steric impediment of the alkyl chains attached to the TTF units and the absence of concentration dependence of the TTF UV−vis−NIR absorption bands suggests that they are caused by intramacromolecular interactions. This hypothesis would indicate that there is at least a certain degree of order in the side chains of the polymer.

Oxidation of the TTF residues in the poly(isocyanide) with bromine and iodine is not as efficient as using $Fe(ClO_4)_3$, although in both cases the position of the UV−vis−NIR absorption bands and their evolution are similar to the oxidation with $Fe(ClO_4)_3$ (see the Supporting Information). Importantly, the band characteristic of MV aggregates (at 2100 nm) was also observed (it presents a maximum after adding 0.5 equiv of Br_2[44]). More equivalents of oxidant are necessary to reach a given state of the polymer and, especially, to generate the dicationic state (Table 2). The halogens do present the advantage of not generating metal salts in the sample and the ability to use a single solvent in the doping process.

The oxidation process can be reversed chemically by the addition of triethylamine. Reduction in this way and subsequent reoxidation with $Fe(ClO_4)_3$ permits full reversibility of the redox reactions and interconversion of the different valence states of the polymer. Figure 7 shows the reversibility of three characteristic bands of the doped states of **6** (the absorption bands at 740 and 930 nm that can be attributed to the TTF cation radical

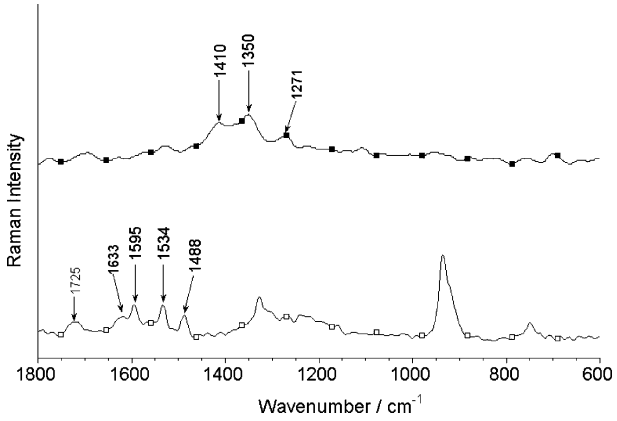

Figure 8. 1064 nm FT-Raman spectra of the neutral (open squares) and oxidized polymer (black squares). Background fluorescence has been removed.

or stacks of it, and the band at 2100 nm that is typical of MV aggregates of neutral and cation radical TTFs) after alternating additions of $Fe(ClO_4)_3$ and NEt_3 to a solution of the neutral polymer.[45]

The FT-IR spectrum of a sample of the poly(isocyanide) doped in solution with 0.5 equiv of $Fe(ClO_4)_3$ and isolated as a powder after evaporation of the solvent displays new and medium intensity bands (the strongest one around 1070 cm^{-1} is due to the perchlorate counteranion) when compared with that of the neutral polymer. The simultaneous appearance of both neutral/oxidized IR (see Supporting Information Figure S5) signals is an indication of a low oxidation regime in the doped material, since the well-known great infrared activity of the oxidation-induced IR bands in the TTF salts is due to electron−vibration coupling.

Laser Raman spectroscopy offers great potential for characterization of organic conducting materials by measuring certain diagnostic vibrations in these salts.[46] The selective enhancement of a few active−symmetric Raman modes due to the large electron−phonon coupling in the TTF-based molecules makes this spectroscopic technique a very sensitive tool, especially for the evaluation of the charge state of the donor. The effect of the positive electrical charge residing on the TTF moiety is to decrease the electron population of its HOMO, whose coefficients are bonding with respect to the C═C bonds. Consequently, the weakening of these bonds leads to lower vibrational frequencies for the Raman-observed lines.

The FT-Raman spectra of the neutral material (Figure 8) is characterized by the occurrence of 4−5 intense scatterings each one arising from symmetric stretching modes of the various functionalities of the pendant monomer. The weak lines at 1725 and 1633 cm^{-1} probably arise from the symmetric C═O and C═N stretching vibrations, respectively.[47] The intense line at 1595 cm^{-1} emerges from the breathing mode or phenyl C−C stretching vibration, whereas the lines at 1534 and 1488 cm^{-1} likely arise from the C═C stretching modes of the TTF moiety, the former due to the oscillation of the outermost TTF C═C bonds (υ_2), and the latter associated with the motion of the central C═C bond (υ_3).[48] In neutral bis(ethylenedithio)-TTF (BEDT-TTF)[49] the υ_2/υ_3 modes appear at 1551/1495 cm^{-1}, whereas in the FT-Raman spectrum of neutral TTF (υ_2/υ_3: 1560/1516 cm^{-1}) these modes appear at higher frequencies than in our polymer. This must be accounted for by the π donor → acceptor interactions (charge transfer) which polarizes the building TTF electronic structure trough the S−C═C−C═O ↔ S^+═C−C−C═O^- conjugated path. This effect is stressed in the case of a TTF-*o*-quinone[50] molecule having a marked

TTF → *o*-quinone charge-transfer feature where the Raman υ_3 frequency is measured at 1446 cm^{-1}, to be compared with that at 1516 cm^{-1} in TTF and at 1488 cm^{-1} in the neutral polymer. These wavenumber differences might be accounted for by the different electron-withdrawing strength of the double C═O functionality in the quinone moiety regarding the single one in the polymer.

The oxidized polymer shows intense near-IR electronic absorptions matching the wavelength of the 1064 nm laser used for the Raman experiments; hence, the recorded spectrum is enhanced by Raman resonance. As a result, the main scattering signals might be linked to Raman-active vibrations associated to the chromophore absorbing at the wavelength of the laser excitation. This spectrum is dominated by two intense and broad lines at 1410 and 1350 cm^{-1}. Previous studies for BEDT-TTF 1:1 salts have shown a systematic displacement at lower frequencies (by ≈80 cm^{-1} for the 1:1 salts) of the symmetric C═C stretching of the TTF moiety.[48] Another feature of the Raman lines of the BEDT-TTF 1:1 salts is the overlapping of their intense lines, such as is observed in the Raman spectrum of our treated polymer. Regarding the wavenumber values, in our case, large downshifts, of 1534 → 1410 cm^{-1} (124 cm^{-1}) and 1488 → 1350 cm^{-1} (138 cm^{-1}), are measured in going from the neutral to the oxidized polymer as compared with the ≈80 cm^{-1} for the neutral BEDT-TTF→BEDT-TTF 1:1 salts. Density functional theory calculations at the B3LYP/3-21G* level have been carried out for a model system (CH_3 instead of $C_{12}HC_{25}$) of the pendant group of the polymer, as neutral and as radical cation (UB3LYP), to support the experimental findings. Model chemistry predicts a downshift of ≈150 cm^{-1} for the strongest theoretical Raman line in passing from the neutral to the oxidized polymer that is correlated with the greatest (138 cm^{-1}) displacement of the frequency of the υ_3 mode. It is reasonably expected that oxidation in the polymer would affect mostly the dithiol group linked to the $SC_{12}HC_{25}$ groups, and consequently its frequency Raman changes upon oxidation might be more marked than in the case of the BEDT-TTF 1:1 salts wherein structural effects upon electron withdrawal is shared by two dithiol groups. The same reasoning applies for the observation of the main scatterings of the oxidized polymer at lower values (1410−1350 cm^{-1}) than those commonly found (≈1460 cm^{-1}) for the BEDT-TTF 1:1 salts. Raman data thus seem to show a scenario for the oxidized system where positive charges prefer to be located at the periphery of the polymeric backbone mitigating more effectively electrostatics repulsions between charges of the same sign in contiguous like-TTF moieties.

EPR measurements were also performed during the oxidation of both the polymer and its precursor **2** with $Fe(ClO_4)_3$.[51] All EPR spectra (which were recorded under the same conditions) showed a signal centered at 2.0071, typical of TTF cation radicals[52] (Figure 9), the only redox form of TTF that is EPR visible. The area of the signal is related with the concentration of the EPR-active species in solution. The plot of the normalized EPR signal area versus the number of oxidant equivalents added to a solution of TTF reference compound **2** (Figure 10) shows a symmetrical curve that starts with low values of EPR signal areas when small amounts of oxidant are added (and the first TTF cation radicals are generated) to increase progressively and reach a maximum after adding ∼1 equiv of iron salt—where all the TTFs are as a cation radical. In contrast, the plot for the oxidation of polymer **6** (Figure 10) displays an unsymmetrical curve with an initial abrupt increase of the EPR signal intensity that has a maximum at 0.5 equiv of oxidant added and decreases in intensity gradually after this point. This contrasting behavior

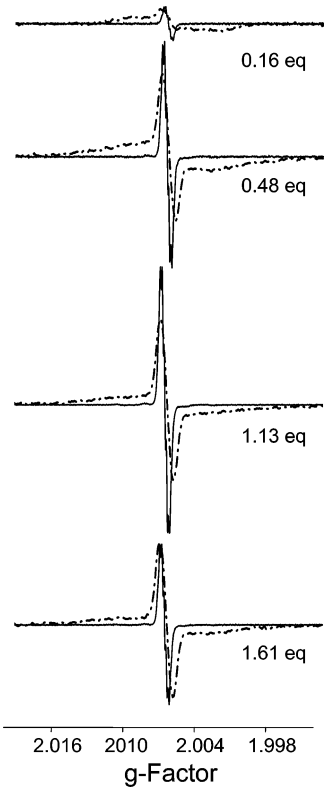

Figure 9. EPR signals of polymer **6** (dot−dash line) and compound **2** (solid line) in CH_2Cl_2/CH_3CN 7:3 at different doping levels of $Fe(ClO_4)_3$.

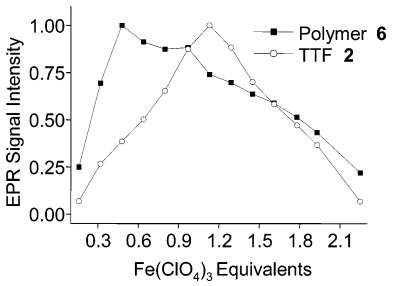

Figure 10. Normalized EPR signal intensity vs no. of equiv of $Fe(ClO_4)_3$ added to polymer **6** and precursor **2** solutions in CH_2Cl_2/CH_3CN.

is due to the presence of magnetic coupling between cation radicals in the side chains of the polymer which results in a decrease in intensity after addition of only 0.5 equiv of oxidant and confirms that the TTF units are close enough to interact in the side chains of the polymer.

At low doping levels the EPR signal of the doped polymer (Figure 9) is comprised of a broad peak and a narrower overlapped signal (with a bandwidth, ΔH_{pp}, of ∼1.95 G and centered at the same point) which becomes more intense as the doping level is increased. Contrarily, the cation radical of compound **2** displays just one signal type, whose bandwidth is of 1.29 G (Figure 9) and presents hyperfine structure due to the coupling of the single electron with the hydrogen atom attached to the TTF unit, the $-SCH_2-$ of the alkyl chains (Figure S8). The polymer's TTF radical signal has a higher line width than **2**, and the hyperfine coupling in the macromolecule cannot be resolved. These differences arise from the distribution of locations of the radicals and the slower tumbling in the polymer. However, the signal line width (SLW) of this polymer is not high and it contrasts with the SLW observed for the wider EPR signal also observed at low doping levels (Figure 11). The

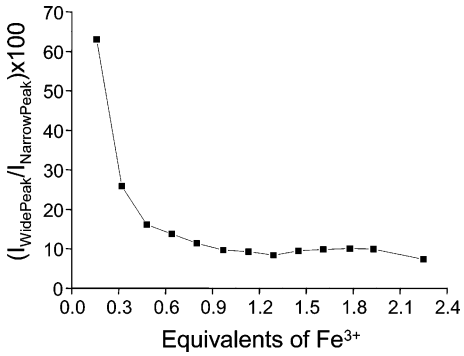

Figure 11. Plot of the relative intensities of the wide and narrow peaks in the EPR spectra of **6** as a function of oxidation degree.

narrowing of the EPR signal as degree of oxidation is increased is most probably caused by an exchange between spins of isolated polarons (isolated cation radicals) and stacks of cation radicals,[53] which does not take place significantly at low doping levels.

Conclusions

The poly(isocyanide) backbone is a useful scaffold for the organization of π-functional units such as the TTFs described here, which are held in close proximity, possibly with the help of van der Waals interactions between the alkyl chains, in a way which is apparently a rigid enough environment that avoids the formation of localized dimers. This arrangement of the π-electron-rich units means that when they are oxidized to form mixed valence states absorption bands are observed which are characteristic of charge transfer between the moieties. The mixed valence state containing cation radicals and neutral TTF residues shows clear evidence of charge transport along the polymer. The easy processing of the material, which is perfectly soluble in a range of solvents, its stability, and versatility make this system an interesting one for the study of electron transport in macromolecules at the nanoscale, since it can be seen as an insulated (with alkyl chains) "nanowire". As it is, with absorption spectroscopy in solution we have shown that the polymer can perform electrochromism, in a distinct way to the monomer system. The indirect link that the poly(isocyanide) backbone provides therefore ensures an adequate separation between the TTF moieties in a macromolecular environment.

Acknowledgment. We thank Judit Orò for the TG measurements, Angel Pérez del Pino and Maria Jesús Polo for the AFM measurements, and Josep Maria Moretó for helpful discussions. This work was supported by the European Integrated Project NAIMO (NMP4-CT-2004-500355), the Programa General de Conocimento of the Dirección General de Investigación, Ciencia y Tecnología (Spain), under the Project CTQ2006-06333/BQU, and the DGR, Catalonia (Project 2005 SGR-00591). E.G.-N. is grateful to the Generalitat de Catalunya for a predoctoral grant. Research at the University of Málaga was supported by the MEC through Project CTQ2006-14987-C02-01 and by the Junta de Andalucia for the Project P06-FQM-01678.

Supporting Information Available: Figures showing IR, ^{1}H NMR, and ^{13}C NMR spectra, CV plots, comparison of IR spectra, a plot of the normalized intensity vs the number of equivalents of Fe^{3+}, EPR spectra, UV−vis−NIR spectra, and FT-NIR spectra. This material is available free of charge via the Internet at http://pubs.acs.org.

References and Notes

(1) (a) Joachim, C.; Gimzewski, J. K.; Aviram, A. *Nature* **2000**, *408*, 541−548. (b) Carroll, R. L.; Gorman, C. B. *Angew. Chem., Int. Ed.* **2002**, *41*, 4378−4400. (c) Maruccio, G.; Cingolani, R.; Rinaldi, R. *J. Mater. Chem.* **2004**, *14*, 542−554.

(2) (a) Tans, S. J.; Verschueren, A. R. M.; Dekker, C. *Nature* **1998**, *393*, 49−52. (b) Rueckes, T.; Kim, K.; Joselevich, E.; Tseng, G. Y.; Cheung, C.-L.; Lieber, C. M. *Science* **2000**, *289*, 94−97. (c) Auvray, S.; Derycke, V.; Goffman, M.; Filoramo, A.; Jost, O.; Bourgoin, J. P. *Nano Lett.* **2005**, *5*, 451−455. (d) Dujardin, E.; Derycke, V.; Goffman, M. F.; Lefevre, R.; Bourgoin, J. P. *Appl. Phys. Lett.* **2005**, *87*, 193107.

(3) (a) Shirakawa, H. *Angew. Chem., Int. Ed.* **2001**, *40*, 2575−2580. (b) MacDiarmid, A. G. *Angew. Chem., Int. Ed.* **2001**, *40*, 2581−2590. (c) Heeger, A. J. *Angew. Chem., Int. Ed.* **2001**, *40*, 2591−2611. (d) *Handbook of Advanced Electronic and Photonic Materials and Devices*−*Conducting Polymers*; Nalwa, H. S., Ed.; Academic Press: London, 2001; Vol. 8. (e) Perepichka, I. F.; Perepichka, D. F.; Meng, H.; Wudl, F. *Adv. Mater.* **2005**, *17*, 2281−2305. (f) Jang, J. *Adv. Polym. Sci.* **2006**, *199*, 189−259. (g) Jaiswal, M.; Menon, R. *Polym. Int.* **2006**, *55*, 1371−1384. (h) Aleshin, A. N. *Adv. Mater.* **2006**, *18*, 17−27.

(4) (a) Schoonbeek, F. S.; van Esch, J. H.; Wegewijs, B.; Rep, D. B. A.; de Haas, M. P.; Klapwijk, T. M.; Kellogg, R. M.; Feringa, B. L. *Angew. Chem., Int. Ed.* **1999**, *38*, 1393−1397. (b) Cavallini, M.; Facchini, M.; Massi, M.; Biscarini, F. *Synth. Met.* **2004**, *146*, 283−286. (c) Schenning, A. P. H. J.; Meijer, E. W. *Chem. Commun.* **2005**, 3245−3258.

(5) (a) O'Neill, M. A.; Barton, J. K. *Top. Curr. Chem.* **2004**, *236*, 67−115. (b) Gorodetsky, A. A.; Barton, J. K. *Langmuir* **2006**, *22*, 7917−7922. (c) Ndlebe, T.; Schuster, G. B. *Org. Biomol. Chem.* **2006**, *4*, 4015−4021. (d) Joseph, J.; Schuster, G. B. *Org. Lett.* **2007**, *9*, 1843−1846.

(6) (a) Sisido, M. *Macromolecules* **1989**, *22*, 4367−4372. (b) Sisido, M.; Reidy, M. P.; Green, M. M. *Macromolecules* **1991**, *24*, 6860−6862. (c) Kuragaki, M.; Sisido, M. *J. Phys. Chem.* **1996**, *100*, 16019−16025. (d) Ikkala, I.; ten Brinke, G. *Chem. Commun.* **2004**, 2131−2137. (e) Tew, G. N.; Aamer, K. A.; Shunmugam, R. *Polymer* **2005**, *46*, 8440−8447. (f) Kato, T.; Mizoshita, N.; Kishimoto, K. *Angew. Chem., Int. Ed.* **2006**, *45*, 38−68. (g) ten Brinke, G.; Ikkala, I. *ACS Symp. Ser.* **2005**, *916*, 34−46. (h) Brettar, J.; Burgi, T.; Donnio, B.; Guillon, D.; Klappert, R.; Scharf, T.; Deschenaux, R. *Adv. Funct. Mater.* **2006**, *16*, 260−267. (i) Kas, O. Y.; Charati, M. B.; Kiick, K. L.; Galvin, M. E. *Chem. Mater.* **2006**, *18*, 4238−4245. (j) Jenekhe, S. A.; Alam, M. M.; Zhu, Y.; Jiang, S. Y.; Shevade, A. V. *Adv. Mater.* **2007**, *19*, 536−542.

(7) (a) Hill, J. P.; Jin, W.; Kosaka, A.; Fukushima, T.; Ichihara, H.; Shimomura, T.; Ito, T.; Hashizume, T.; Ishii, N.; Aida, T. *Science* **2004**, *304*, 1481−1483. (b) Grimsdale, A. C.; Müllen, K. *Angew. Chem., Int. Ed.* **2005**, *44*, 5592−5629.

(8) (a) Fuhrhop, J. H.; Demoulin, C.; Boettcher, C.; Köning, J.; Siggel, U. *J. Am. Chem. Soc.* **1992**, *114*, 4159−4165. (b) Bindig, U.; Schulz, A.; Fuhrhop, J. H.; Siggel, U. *New J. Chem.* **1995**, *19*, 427−435. (c) Warman, J. M.; Kroeze, J. E.; Schouten, P. G.; van de Craats, A. M. *J. Porphyrins Phthalocyanines* **2003**, *7*, 342−350. (d) Elemans, J. A. A. W.; Nolte, R. J. M.; Rowan, A. E. *J. Porphyrins Phthalocyanines* **2003**, *7*, 249−254. (e) Schwab, A. D.; Smith, D. E.; Bond-Watts, B.; Johnston, D. E.; Hone, J.; Johnson, A. T.; de Paula, J. C.; Smith, W. F. *Nano Lett.* **2004**, *4*, 1261−1265. (f) Takeuchi, M.; Tanaka, S.; Shinkai, S. *Chem. Commun.* **2005**, 5539−5541.

(9) (a) Kobayashi, N.; Lever, A. B. P. *J. Am. Chem. Soc.* **1987**, *109*, 7433−7448. (b) van Nostrum, C. F.; Picken, S. J.; Nolte, R. J. M. *Angew. Chem., Int. Ed. Engl.* **1994**, *33*, 2173−2175. (c) Fox, J. M.; Katz, T. J.; Van Elschocht, S.; Verbiest, T.; Kauranen, M.; Persoons, A.; Thongpanchang, T.; Krauss, T.; Brus, L. *J. Am. Chem. Soc.* **1999**, *121*, 3453−3459. (d) Guldi, D. M.; Gouloumis, A.; Vázquez, P.; Torres, T.; Georgakilas, V.; Prato, M. *J. Am. Chem. Soc.* **2005**, *127*, 5811−5813. (e) Sly, J.; Kasák, P.; Gomar-Nadal, E.; Rovira, C.; Górriz, L.; Thordarson, P.; Amabilino, D. B.; Rowan, A. E.; Nolte, R. J. M. *Chem. Commun.* **2005**, 1255−1257. (f) Sergeyev, S.; Pouzet, E.; Debever, O.; Levin, J.; Gierschner, J.; Cornil, J.; Gómez-Aspe, R.; Geerts, Y. H. *J. Mater. Chem.* **2007**, *17*, 1777−1784.

(10) Crispin, X.; Cornil, J.; Friedlein, R.; Okudaira, K. K.; Lemaur, V.; Crispin, A.; Kestemont, G.; Lehman, M.; Fahlman, M.; Lazzaroni, R.; Geerts, Y.; Wendin, G.; Ueno, N.; Brédas, J.-L.; Salaneck, W. R. *J. Am. Chem. Soc.* **2004**, *126*, 11889−11899.

(11) (a) Hanack, M.; Lang, M. *Adv. Mater.* **1994**, *6*, 819−833. (b) Prins, P.; Senthilkumar, K.; Grozema, F. C.; Jonkheijm, P.; Schenning, A. P. H. J.; Meijer, E. W.; Siebbeles, L. D. A. *J. Phys. Chem. B* **2005**, *109*, 18267−18274. (c) An, Z. S.; Yu, J. S.; Jones, S. C.; Barlow, S.; Yoo, S.; Domercq, B.; Prins, P.; Siebbeles, L. D. A.; Kippelen, B.; Marder, S. R. *Adv. Mater.* **2005**, *17*, 2580−2583.

(12) For general reviews about TTFs, see: (a) Nielsen, M. B.; Lomholt, C.; Becher, J. *Chem. Soc. Rev.* **2000**, *29*, 153−164. (b) Bryce, M. R. *J. Mater. Chem.* **2000**, *10*, 589−598. (c) Segura, J. L.; Martín, N. *Angew. Chem., Int. Ed.* **2001**, *40*, 1372−1406. (d) Schukat, G.; Fanghänel, E. *Sulfur Rep.* **2003**, *24*, 1−190. (e) Yamada, J.-I., Sugimoto, T., Eds. *TTF Chemistry: Fundamentals and Applications of Tetrathiafulvalene*; Springer-Verlag: Berlin, 2004. (f) Gorgues, A. *J. Phys. IV* **2004**, *114*, 405−410. For recent examples and references therein, see: (g) Hasegawa, M.; Enozawa, H.; Kawabata, Y.; Iyoda, M. *J. Am. Chem. Soc.* **2007**, *129*, 3072−3073. (h) Savy, J. P.; de Caro, D.; Faulmann, C.; Valade, L.; Almeida, M.; Koike, T.; Fujiwara, H.; Sugimoto, T.; Fraxedas, J.; Ondarcuhu, T.; Pasquier, C. *New J. Chem.* **2007**, *31*, 519−527. (i) Fang, C.-J.; Zhu, Z.; Sun, W.; Xu, C.-H.; Yan, C.-H. *New J. Chem.* **2007**, *31*, 580−586.

(13) Charge-transfer salts and complexes of tetrathiafulvalenes: (a) Bryce, M. R. *Chem. Soc. Rev.* **1991**, *20*, 355−390. (b) Khodorkovsky, V.; Becker, J. Y. In *Organic Conductors*; Farges, J.-P., Ed.; Marcel Dekker: New York, 1994; Chapter 3. (c) Yamada, J.; Akutsu, H.; Nishikawa, H.; Kikuchi, K. *Chem. Rev.* **2004**, *104*, 5057−5083. (d) Geiser, U.; Schlueter, J. A. *Chem. Rev.* **2004**, *104*, 5203−5241. (e) Fourmigue, M.; Batail, P. *Chem. Rev.* **2004**, *104*, 5379−5481. (f) Mori, H. *J. Phys. Soc. Jpn.* **2006**, *75*, 051003.

(14) (a) Rovira, C. *Chem. Rev.* **2004**, *104*, 5289−5317. (b) Mas-Torrent, M.; Rovira, C. *J. Mater. Chem.* **2006**, *16*, 433−436. (c) Gao, X. K.; Wu, W. P.; Liu, Y. Q.; Jiao, S. B.; Qiu, W. F.; Yu, G.; Wang, L. P.; Zhu, D. *J. Mater. Chem.* **2007**, *17*, 736−743.

(15) (a) Kitamura, T.; Nakaso, S.; Mizoshita, N.; Tochigi, Y.; Shimomura, T.; Moriyama, M.; Ito, K.; Kato, T. *J. Am. Chem. Soc.* **2005**, *127*, 14769−14775. (b) Kitahara, T.; Shirakawa, M.; Kawano, S.-i.; Beginn, U.; Fujita, N.; Shinkai, S. *J. Am. Chem. Soc.* **2005**, *127*, 14980−14981. (c) Wang, C.; Zhang, D.; Zhu, D. *J. Am. Chem. Soc.* **2005**, *127*, 16372−16373. (d) Akutagawa, T.; Kakiuchi, K.; Hasegawa, T.; Noro, S.-i.; Nakamura, T.; Hasegawa, H.; Mashiko, S.; Becher, J. *Angew. Chem., Int. Ed.* **2005**, *44*, 7283−7287. (e) Puigmartí-Luis, J.; Laukhin, V.; Pérez del Pino, A.; Vidal-Gancedo, J.; Rovira, C.; Laukhina, E.; Amabilino, D. B. *Angew. Chem., Int. Ed.* **2007**, *46*, 238−241.

(16) (a) Millich, F. *J. Polym. Sci., Macromol. Rev.* **1980**, *15*, 207−253. (b) Nolte, R. J. M. *Chem. Soc. Rev.* **1994**, *23*, 11−19. (c) Cornelissen, J. J. L.; Rowan, A. E.; Nolte, R. J. M.; Sommerdijk, N. A. J. M. *Chem. Rev.* **2001**, *101*, 4039−4070.

(17) Hernando, J.; De Witte, P. A. J.; van Dijk, E. M. H. P.; Korterik, J.; Nolte, R. J. M.; Rowan, A. E.; García-Parajó, M. F.; van Hulst, N. F. *Angew. Chem., Int. Ed.* **2004**, *43*, 4045−4049.

(18) (a) Takei, F.; Hayashi, H.; Onitsuka, K.; Kobayashi, N.; Takahashi, S. *Angew. Chem., Int. Ed.* **2001**, *40*, 4092−4094. (b) Goto, H.; Yashima, E. *J. Am. Chem. Soc.* **2002**, *124*, 7943−7949. (c) Hida, N.; Takei, F.; Onitsuka, K.; Shiga, K.; Asoaka, S.; Iyoda, T.; Takahashi, S. *Angew. Chem., Int. Ed.* **2003**, *42*, 4349−4352. (d) De Witte, P. A. J.; Castriciano, M.; Cornelissen, J. J. L. M.; Scolaro, L. M.; Nolte, R. J. M.; Rowan, A. E. *Chem. Eur. J.* **2003**, *9*, 1775−1781. (e) Amabilino, D. B.; Serrano, J.-L.; Sierra, T.; Veciana, J. *J. Polym. Sci., Part A: Polym. Chem.* **2006**, *44*, 3161−3174. (f) Hase, Y.; Ishikawa, M.; Muraki, R.; Maeda, K.; Yashima, E. *Macromolecules* **2006**, *39*, 6003−6008.

(19) (a) Kollmar, C.; Hoffmann, R. *J. Am. Chem. Soc.* **1990**, *112*, 8230−8238. (b) Cui, C.-X.; Kertesz, M. *Chem. Phys. Lett.* **1990**, *169*, 445−449. (c) Clericuzio, M.; Alagona, G.; Ghio, C.; Salvadori, P. *J. Am. Chem. Soc.* **1997**, *119*, 1059−1071.

(20) Kajitani, T.; Okoshi, K.; Sakurai, S.-i.; Kumaki, J.; Yashima, E. *J. Am. Chem. Soc.* **2006**, *128*, 708−709.

(21) (a) Hertler, W. R. *J. Org. Chem.* **1976**, *41*, 1412−1416. (b) Pittman, C. U., Jr.; Liang, Y.-F.; Ueda, M. *Macromolecules* **1979**, *12*, 355−359. (b) Wang, E.; Li, H.; Hu, W.; Zhu, D. *J. Polym. Sci., Part A: Polym. Chem.* **2006**, *44*, 2707−2713. (c) Frenzel, S.; Baumgarten, M.; Mullen, K. *Synth. Met.* **2001**, *118*, 97−103.

(22) (a) Lyskawa, J.; Le Derf, F.; Levillian, E.; Mazzari, M.; Salle, M.; Dubois, L.; Viel, P.; Bureau, C.; Palacin, S. *J. Am. Chem. Soc.* **2004**, *126*, 12194−12195. (b) Shimada, S.; Masaki, A.; Hayamizu, K.; Matsuda, H.; Okada, S.; Nakanishi, H. *Chem. Commun.* **1997**, 1421−1422. (c) Shimizu, T.; Yamamoto, T. *Chem. Commun.* **1999**, 515−516. (d) Huchet, L.; Akoudad, S.; Roncali, J. *Adv. Mater.* **1998**, *10*, 541−545.

(23) (a) Wu, P.; Saito, G.; Imaeda, K.; Shi, Z.; Mori, T.; Enoki, T.; Inokuchi, H. *Chem. Lett.* **1986**, 441−444. (b) Inokuchi, H.; Saito, G.; Wu, P.; Seki, K.; Tang, T. B.; Mori, T.; Imaeda, K.; Enoki, T.; Higuchi, Y.; Inaka, K.; Yasouka, N. *Chem. Lett.* **1986**, 1263−1266. (c) Ukai, S.; Igarashi, S.; Nakajima, M.; Marumoto, K.; Ito, H.; Kuroda, S.; Nishimura, K.; Enomoto, Y.; Saito, G. *Colloids Surf., A* **2006**, *284−285*, 589−593.

(24) Gomar-Nadal, E.; Veciana, J.; Rovira, C.; Amabilino, D. B. *Adv. Mater.* **2005**, *17*, 2095−2098.

(25) Kim, M.; Euler, W. B.; Rossen, W. *J. Org. Chem.* **1997**, *62*, 3766−3769.

(26) González, M.; Martín, N.; Segura, J. L.; Garín, J.; Orduna, J. *Tetrahedron Lett.* **1998**, *39*, 3269−3272.

(27) The NMR of the formanilide derivative (**4**) described here is complicated by the presence of unequal populations of the cis and trans isomers about the amide bond, a phenomenon noted previously: Bourn, A. J. R.; Gillies, D. G.; Randall, E. W. *Tetrahedron* **1964**, *20*, 1811−1818. This asymmetry vanishes from the NMR spectrum upon conversion of the formamide to the isocyanide.

(28) (a) Deming, T. J.; Novak, B. M. *Macromolecules* **1993**, *26*, 7092−7094. (b) Deming, T. J.; Novak, B. M. *J. Am. Chem. Soc.* **1993**, *115*, 9101−9111. (c) Euler, W. B.; Huang, J.-T.; Kim, M.; Spencer, L.; Rosen, W. *Chem. Commun.* **1997**, 257−258.

(29) Amabilino, D. B.; Ramos, E.; Serrano, J.-L.; Sierra, T.; Veciana, J. *Polymer* **2005**, *46*, 1507−1521.

(30) Supposing a 4_1 helical structure, with a pitch of 4 Å, and using the molecular weight determined by GPC.

(31) (a) Cornelissen, J. J. L. M.; Donners, J. J. J. M.; de Gelder, R.; Graswinckel, W. S.; Metselaar, G. A.; Rowan, A. E.; Sommerdijk, N. A. J. M.; Nolte, R. J. M. *Science* **2001**, *293*, 676−680. (b) Metselaar, G. A.; Wezenberg, S. J.; Cornelissen, J. J. L. M.; Nolte, R. M.; Rowan, A. E. *J. Polym. Sci., Part A: Polym. Chem.* **2007**, *45*, 981−988. (c) Metselaar, G. A.; Adams, P. J. H. M.; Nolte, R. J. M.; Cornelissen, J. J. L. M.; Rowan, A. E. *Chem. Eur. J.* **2007**, *13*, 950−960.

(32) (a) Wegner, G. *Acta Mater.* **2000**, *48*, 253−262. (b) Ober, C. K. *Science* **2000**, *288*, 448−449.

(33) Ishikawa, M.; Maeda, K.; Yashima, E. *J. Am. Chem. Soc.* **2002**, *124*, 7448−7458.

(34) Hu, D.; Yu, J.; Wong, K.; Bagchi, B.; Rossky, P. J.; Barbara, P. F. *Nature* **2000**, *405*, 1030−1033.

(35) (a) Millich, F.; Baker, G. K. *Macromolecules* **1969**, *2*, 122−128. (b) Pini, D.; Iuliano, A.; Salvadori, P. *Macromolecules* **1992**, *25*, 6059−6062. (c) Green, M. K.; Gross, R. A.; Schilling, F. C.; Zero, K.; Crosby, C., III. *Macromolecules* **1998**, *21*, 1839−1846. (d) Spencer, L.; Kim, M.; Euler, W. B.; Rosen, W. *J. Am. Chem. Soc.* **1997**, *119*, 8129−8130. (e) Huang, J.-T.; Sun, J.; Euler, W. B.; Rosen, W. *J. Polym. Sci., Part A: Polym. Chem.* **1997**, *35*, 439−446. (f) Ishikawa, M.; Maeda, K.; Mitsutsuji, Y.; Yashima, E. *J. Am. Chem. Soc.* **2004**, *126*, 732−733.

(36) (a) Torrance, J. B. *Acc. Chem. Res.* **1979**, *12*, 79−86. (b) Williams, J. M.; Ferraro, J. R.; Thorn, R. J.; Carlson, K. D.; Geiser, U.; Wang, H. H.; Kini, A. M.; Whangbo, M. H. *Organic Superconductors (Including Fullerenes*); Prentice Hall: Englewoods Cliffs, NJ, 1992.

(37) Formamide **4** was used as reference instead of the monomer **5** because isocyanides may adsorb to the metals present in the electrodes.

(38) Huchet, L.; Akoudad, S.; Levillain, E.; Roncali, J.; Emge, A.; Bäuerle, P. *J. Phys. Chem. B* **1998**, *102*, 7776−7781.

(39) For a general review about chemical redox agents see: Connelly, N. G.; Geiger, W. E. *Chem. Rev.* **1996**, *96*, 877−910.

(40) Torrance, J. B.; Scott, B. A.; Welber, B.; Kaufman, F. B.; Seiden, P. E. *Phys. Rev. B* **1979**, *19*, 730−741.

(41) Addition of 0.5 mol of $Fe(ClO_4)_3$/0.5 mol of TTF unit, considering the molecular weight of the monomer. The Fe(III) salt was titrated as ferric acetate in water prior to use, see: Perrin, D. D. *J. Chem. Soc.* **1959**, *31*, 1181−1182.

(42) For references on calculated and experimental UV−vis absorption of cation radical and dication of TTF derivatives, see: (a) Khodorkovsky, V.; Shapiro, L.; Krief, P.; Shames, A.; Mabon, G.; Gorgues, A.; Giffard, M. *Chem. Commun.* **2001**, 2736−2737. (b) Andreu, R.; Garín, J.; Orduna, J. *Tetrahedron* **2001**, *57*, 7883−7887. (c) Wartelle, C.; Viruela, R.; Viruela, P. M.; Sauvage, F. X.; Sallé, M.; Ortí, E.; Levillain, E.; Le Derf, F. *Phys. Chem. Chem. Phys.* **2003**, *5*, 4672−4679.

(43) (a) Hasegawa, M.; Takano, J.-i.; Enozawa, H.; Kuwatani, Y.; Iyoda, M. *Tetrahedron Lett.* **2004**, *45*, 4109−4112. (b) Ziganshina, A. Y.; Ko, Y. O.; Jeon, W. S.; Kim, K. *Chem. Commun.* **2004**, 806−807. (c) Yoshizawa, M.; Kumazawa, K.; Fujita, M. *J. Am. Chem. Soc.* **2005**, *127*, 13456−13457. (d) Lyskawa, J.; Sallé, M.; Balandier, J.-Y.; Le Derf, F.; Levillain, E.; Allain, M.; Viel, P.; Palacin, S. *Chem. Commun.* **2006**, 2233−2235.

(44) We consider that in 1 equiv of X_2 are 3 mols of X^- taking into account that these reactions happen in solution during the oxidation process: (i) $X_2 + 2e^- \rightarrow 2X^-$ and (ii) $X_2 + X^- \rightarrow X^{3-}$ where X = Br or I. See Mas-Torrent, M.; Ribera, E.; Tkacheva, V.; Mata, I.; Molins, E.; Vidal-Gancedo, J.; Khasanov, S.; Zorina, L.; Shibaeva, R.; Wojciechowski, R.; Ulanski, J.; Wurst, K.; Veciana, J.; Laukhin, V.; Canadell, E.; Laukhina, E.; Rovira, C. *Chem. Mater.* **2002**, *14*, 3295−3304.

(45) Triethylamine is a weak reductant (irreversible peak potential, E_p = +0.47 V in CH_3CN: (a) Nelsen, S. F.; Hintz, P. J. *J. Am. Chem. Soc.*

1972, *94*, 7114), whose oxidation byproducts have not been established. See also (b) Connelly, N. G.; Geiger, E. *Chem. Rev.* **1996**, *96*, 877−910.

(46) (a) Meneghetti, M.; Bozio, R.; Pecile, C. *J. Phys.* **1986**, *47*, 1377−1387. (b) Sugai, S.; Mori, H.; Yamochi, H.; Saito, G. *Phys. Rev. B: Condens. Matter*. **1993**, *47*, 14374−14379.

(47) Sverdlov, L. M.; Kovner, M. A.; Krainov, E. P. *Vibrational Spectra of Polyatomic Molecules*; John Wiley & Sons: Chichester, U.K., 1974.

(48) Drozdova, O.; Yamochi, H.; Yakushi, K.; Uuichi, M.; Horiuchi, S.; Saito, G. *J. Am. Chem. Soc.* **2000**, *122*, 4436−4442.

(49) (a) Wang, H. H.; Ferraro, J.; Willians, J. M.; Geiser, U.; Schlueter, J. A. *J. Chem. Soc., Chem. Commun.* **1994**, 1893−1894. (b) Noh, D.-Y.; Willing, G. A.; Han, C. Y.; Shin, K.-S.; Geiser, U.; Wang, H. H. *Chem. Mater.* **2004**, *16*, 4777−4782.

(50) Dumur, F.; Gautier, N.; Gallego-Planas, N.; Sahin, Y.; Levillain, E.; Mercier, N.; Hudhomme, P.; Masino, M.; Girlando, A.; Lloveras, V.; Vidal-Gancedo, J.; Veciana, J.; Rovira, C. *J. Org. Chem.* **2004**, *69*, 2164−2177.

(51) TTF reference compound **2** was used for the EPR studies instead of precursor **4** because its oxidation potentials are similar to those of **4** and polymer **6** and it has no potentially hydrogen-bond-forming groups (hydrogen-bonded dimers could affect the shape of the EPR signal in compounds such as **4**).

(52) (a) Cavara, L.; Gerson, F.; Cowan, D. O.; Lerstrup, L. *Helv. Chim. Acta* **1986**, *69*, 141−151. (b) Rovira, C.; Veciana, J.; Santaló, N.; Tarrés, J.; Cirujeda, J.; Molins, E.; Llorca, J.; Espinosa, E. *J. Org. Chem.* **1994**, *59*, 3307−3313.

(53) Harima, Y.; Kunugi, Y.; Tang, H.; Yamashita, K.; Shiotani, M.; Ohshita, J.; Kunai, A. *Synth. Met.* **2000**, *113*, 173−183.

MA0710986